

# Structure of Neutron-Rich Nuclei

W. Nazarewicz<sup>1-3</sup> and M. Płoszajczak<sup>4</sup>

<sup>1</sup> *Department of Physics and Astronomy, The University of Tennessee,  
Knoxville, Tennessee 37996, USA*

<sup>2</sup> *Physics Division, Oak Ridge National Laboratory,  
P.O. Box 2008, Oak Ridge, TN 37831, USA*

<sup>3</sup> *Institute of Theoretical Physics, Warsaw University,  
ul. Hoża 69, PL-00681 Warszawa, Poland*

<sup>4</sup> *Grand Accélérateur National d'Ions Lourds (GANIL),  
CEA/DSM – CNRS/IN2P3, BP 55027,  
F-14076 Caen Cedex 05, France*

## Abstract

Structure of exotic radioactive nuclei having extreme neutron-to-proton ratios is different from that around the stability line. This short review discusses the progress in modeling of exotic nuclei in the nuclear “Terra Incognita”. The consistent theoretical description of weakly bound systems requires a synergy between nuclear structure and nuclear reaction methods.

## 1 Introduction

Low-energy nuclear physics is undergoing a renaissance. Experimentally, there has been a technological revolution in the radioactive nuclear beam (RNB) experimentation. The next-generation tools invite us on the journey to the vast territory of nuclear landscape which has never been explored by science. Hand in hand with experimental developments, a qualitative change in theoretical modeling is taking place. Due to the progress in computer technologies and numerical algorithms, it has become exceedingly clear that the unified microscopic understanding of the nuclear many-body system is no longer a dream.

During recent years, we have witnessed substantial progress in many areas of theoretical nuclear structure. Effective field theory offers hope for a link between QCD and nucleon-nucleon forces. New interactions have been developed which, together with a powerful suite of *ab-initio* approaches, provide a quantitative description of light nuclei. For heavy systems, *global* modern shell-model approaches and self-consistent mean-field methods offer a level of

accuracy typical of phenomenological approaches based on parameters *locally* fitted to the data. By exploring connections between models in various regions of the chart of the nuclides, nuclear theory aims to develop a comprehensive, unified theory of the nucleus across the entire nuclear landscape.

From a theoretical point of view, short-lived exotic nuclei far from stability with “abnormal” neutron-to-proton ratios offer a unique test of those aspects of the many-body theory that depend on the isospin degrees of freedom [1]. The challenge to microscopic theory is to develop methodologies to reliably calculate and understand the origins of unknown properties of new physical systems, physical systems with the same ingredients as familiar ones but with totally new and different properties. The hope is that after probing the limits of extreme isospin, we can later go back to the valley of stability and improve the description of normal nuclei.

## 2 Nuclear structure theory: questions and challenges

Theoretical nuclear structure deals with the nuclear many-body problem in the very finite limit of particle number. In the non-relativistic limit, the goal is to solve the many-body Schrödinger equation with the nuclear Hamiltonian  $\hat{H}$ :

$$\hat{H}\Psi = E\Psi. \quad (1)$$

Unlike other areas of the many-body problem (atomic physics, condensed matter physics), nuclear physics is still struggling to understand the origin of the inter-nucleonic force which produces nuclear binding. Although it is clear that the nucleon-nucleon (NN) interaction has its roots in quark-gluon dynamics, the microscopic derivation is not yet in place. In addition, due to strong in-medium effects, additional complications arise when one tries to derive the *effective* interaction in the heavy nucleus. This brings us to the first major scientific question pertaining to Eq. (1): *What is the effective nuclear Hamiltonian?* In this context, some specific issues related to the RNB experimentation are: What is the  $(N - Z)$  and  $A$  dependence (i.e., isovector and isoscalar density dependence) of the effective NN interaction? What is the NN interaction dependence on spin degrees of freedom? What is the nuclear matter equation of state?

In this context, significant progress in the area of the bare nucleon-nucleon force [2] is worth noting. In addition to several excellent phenomenological NN forces (both non-local and local) fitted to the two-body data, new interactions have been obtained in the framework of chiral perturbation theory (or low-momentum expansion) [3, 4]. In addition, three-nucleon forces have been

derived in the chiral effective field theory [5]. The chiral forces are highly nonlocal; hence it is difficult to use them in ab-initio quantum Monte Carlo calculations [6].

The second major challenge pertaining to Eq. (1) – *What is the nature of the nucleonic matter?* – concerns the properties of the many-body wave function  $\Psi$ . Here, the specific fundamental questions are: What is the microscopic mechanism of nuclear binding? Which combinations of protons and neutrons make up a nucleus? What is the single-nucleonic motion in a very neutron-rich environment? What are the collective phases of nucleonic matter? What is the nature of the collective modes of the nucleus (a finite fermion system having a pronounced surface)? What are the relevant collective degrees of freedom? How to understand microscopically the large-amplitude nuclear collective motion (fusion, fission, coexistence phenomena)? Most of these questions are not new. Still, the microscopic answer is missing.

### 3 The territory of nucleonic matter

Figure 1 shows the vast territory of various domains of nuclear matter characterized by the neutron excess,  $(N - Z)/A$ , and the isoscalar nucleonic density ( $\rho = \rho_n + \rho_p$ ). In this diagram, the region of finite (i.e., particle-bound) nuclei extends from the neutron excess of about  $-0.2$  (proton drip line) to  $0.5$  (neutron drip line). The next-generation RNB facilities will provide a unique capability for accessing the very asymmetric nuclear matter and for compressing neutron-rich matter approaching density regimes important for supernova and neutron star physics that are indicated in Fig. 1.

Measurements of neutron skin and radii at RNB facilities will enable us to build an intellectual bridge between finite nuclei and bulk nucleonic matter. Indeed, the thickness of the skin in a heavy nucleus depends on the pressure of neutron-rich matter. The same pressure supports a neutron star against gravity. Thus, models with thicker neutron skins often produce neutron stars with larger radii [8] (see also Ref. [9]). This suggests an inverse relationship: the thicker the neutron-rich skin of a heavy nucleus, the thinner the solid crust of a neutron star. It is an extrapolation of 18 orders of magnitude from the neutron radius of a heavy nucleus (several fm) to the approximately 10 km radius of a neutron star. Yet both radii depend on our incomplete knowledge of the density functional of the neutron-rich matter.

The nuclear equation of state (EOS) describes the possibility of compressing nuclear matter. It plays a central role in nuclear structure and in heavy ion collisions. It also determines the static and dynamical behavior of stars,

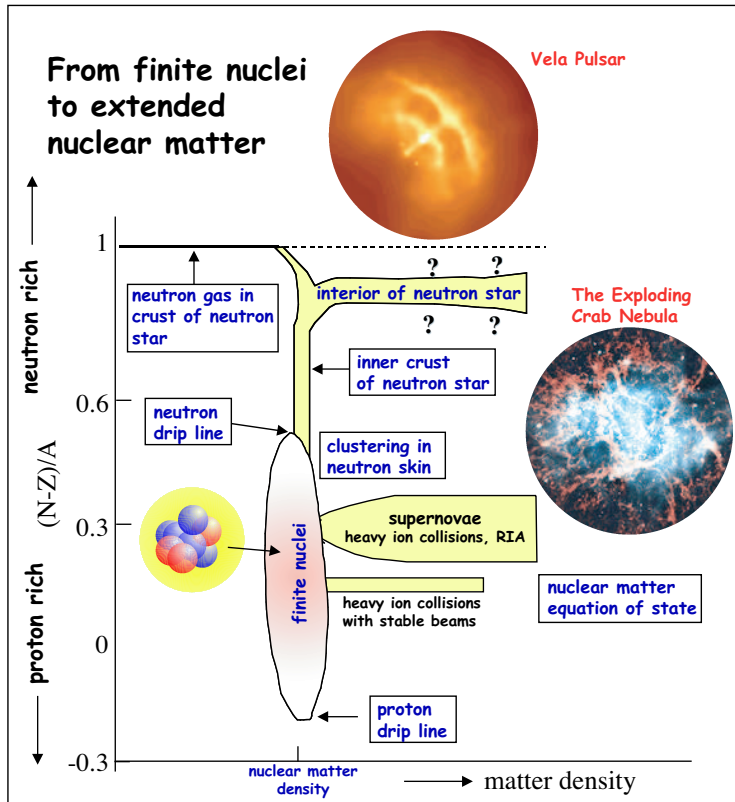


Figure 1: Diagram illustrating the range of nucleonic densities and neutron excess of importance in various contexts of the low- and intermediate-energy nuclear many-body problem. The territory of various domains of nucleonic matter is characterized by the neutron excess and the nucleonic density. The full panoply of bound nuclei comprises the vertical ellipse. Densities accessible with different reactions, and the properties of neutron star layers, are indicated. The new-generation RNB facilities will provide a unique capability for accessing very neutron-rich nuclei – our best experimentally accessible proxies for the bulk neutron-rich matter in the neutron star crust. They will also enable us to compress neutron-rich matter in order to explore the nuclear matter equation of state – essential for the understanding of supernovae and neutron stars. (Based on Ref. [7].)

especially in supernova explosions and in neutron star stability and evolution. Unfortunately, our knowledge of the EOS, especially at high densities and/or temperatures, is very poor. In nuclear collisions at RIA induced by neutron-rich nuclei, a transient state of nuclear matter with an appreciable neutron-to-proton asymmetry, as well as large density, can be created. This will offer the unique opportunity to study the  $N/Z$ -dependence of the EOS, crucial for the supernova problem.

### 3.1 How to extrapolate to neutron-rich matter

Unfortunately, the theoretical knowledge of the equation of state of pure neutron matter is poor; the commonly used energy-density functionals give different predictions for neutron matter. Figure 2 illustrates difficulties with making

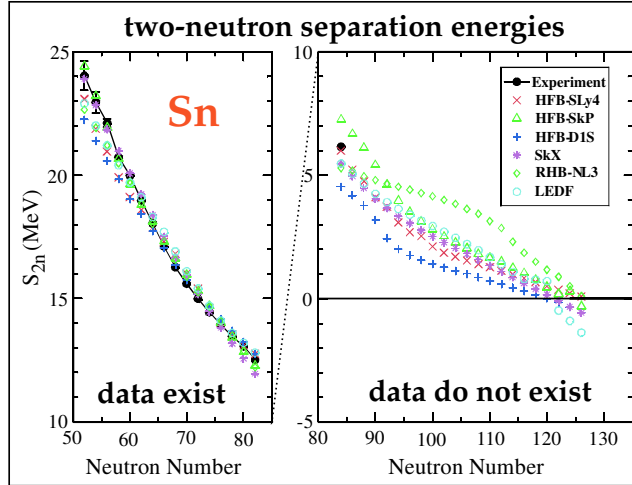


Figure 2: Predicted two-neutron separation energies for the even-even Sn isotopes using several microscopic models based on effective nucleon-nucleon interactions and obtained with phenomenological mass formulas (shown in the inset at top right). (Taken from Ref. [10].)

theoretical extrapolations into neutron-rich territory. It shows the two-neutron separation energies for the even-even Sn isotopes calculated in several microscopic models based on different effective interactions. Clearly, the differences between forces are greater in the neutron-rich region than in the region where masses are known. Therefore, the uncertainty due to the largely unknown isospin dependence of the effective force (in both particle-hole and particle-particle channels) gives an appreciable theoretical “error bar” for the position of the drip line. Unfortunately, the results presented in Fig. 2 do not tell us much about which of the forces discussed should be preferred since one is dealing with dramatic extrapolations far beyond the region known experimentally. However, a detailed analysis of the force dependence of results may give us valuable information on the relative importance of various force parameters.

Many insights can be obtained from microscopic calculations of neutron matter using realistic nucleon-nucleon two-body and three-body forces [11, 12]. These calculations demonstrate that, due to the large nn scattering length, the nuclear energy density functional must diverge at low densities (contrary to

what is used in current self-consistent calculations). This result will certainly be helpful when constraining realistic energy density functionals.

Another difficulty when extrapolating from finite nuclei to the extended nuclear matter is due to the diffused neutron surface in neutron-rich nuclei. As discussed in Ref. [13], the nuclear surface cannot simply be regarded as a *layer of nuclear matter at low density*. In this zone the gradient terms (absent in the nuclear matter) are as important in defining the energy relations as those depending on the local density.

## 4 Self-consistent mass table

Self-consistent methods based on density-dependent effective interactions have achieved a level of sophistication and precision which allows analyses of experimental data for a wide range of properties and for arbitrarily heavy nuclei. For instance, a self-consistent *deformed* mass table has been recently developed [14] based on the Skyrme energy functional. The resulting rms error on binding energies of 1700 nuclei is around several hundred keV, i.e., is comparable with the agreement obtained in the shell-correction approaches.

Microscopic mass calculations require a simultaneous description of particle-hole, pairing, and continuum effects – the challenge that only very recently could be addressed by mean-field methods. Very recently we have developed methods [15] to approach the problem of large-scale deformed HFB calculations by using the local-scaling point transformation [16, 17] that allows us to modify asymptotic properties of the deformed harmonic oscillator wave functions. Such calculations can be optimized to take advantage of parallel computing. (For example, it takes only one day to calculate the full self-consistent even-even mass table considering prolate, oblate, and spherical shapes!) Our large-scale mass calculations will take into account a number of improvements:

- Implementation of the exact particle number projection before variation [18, 19].
- Improvement of the density dependence of the effective interaction, including: (i) better treatment of the low-density dependence [12], (ii) corrections beyond the mean-field and three-body effects [20], and (iii) the surface-peaked effective mass [21].
- Proper treatment of the time-odd fields [22].
- Inclusion of dynamical zero-point fluctuations associated with the nuclear collective motion [23, 24].

The resulting universal energy density functional will be fitted to nuclear masses, radii, giant vibrations, and other global nuclear characteristics.

## 5 Continuum shell-model

The major theoretical challenge in the microscopic description of weakly bound nuclei is the rigorous treatment of both the many-body correlations and the continuum of positive-energy states and decay channels. Weakly bound states or resonances cannot be described within the closed quantum system formalism. For bound states, there appears a virtual scattering into the continuum phase space involving intermediate scattering states. Continuum coupling of this kind affects also the effective nucleon-nucleon interaction. For unbound states, the continuum structure appears explicitly in the properties of those states. The consistent treatment of continuum in multi-configuration mixing calculations is the domain of the continuum shell model (CSM) (see Ref. [25] for a review).

The impact of the particle continuum was discussed in the early days of the multiconfigurational SM in the middle of the last century. However, thanks to the success of the ‘standard’ SM in terms of interacting nucleons (assumed to be *perfectly isolated* from an *external environment* of scattering states), the continuum-related matters had been swept under the rug. An example of a problem is the so-called Thomas-Ehrman shift [26] appearing in, e.g., the mirror nuclei  $^{13}\text{C}$ ,  $^{13}\text{N}$ , which is a salient effect of a coupling to the continuum depending on the position of the respective particle emission thresholds. In the following, we discuss two recent developments in the area of the CSM.

### 5.1 Shell-Model Embedded in the Continuum

In the Shell Model Embedded in the Continuum (SMEC) [27, 25], all coupling matrix elements between different discrete states, different scattering states, as well as between discrete and scattering states, are calculated using the realistic effective SM interaction. Below, we discuss certain features of the coupling to the particle continuum in the example of binding energy systematics.

In SMEC, the localized many-body states forming a  $Q$ -subspace are obtained by solving a standard SM problem for the Hamiltonian  $H_{QQ}$ . Asymptotic channels made of  $(A - 1)$ -particle localized states and one nucleon in the scattering state are contained in  $P$ -subspace. The residual coupling ( $H_{PQ}$ ) between these two subspaces is given by the zero-range interaction including the spin-exchange term. An effective Hamiltonian including the coupling to

the continuum is energy-dependent:

$$\mathcal{H}(E) = H_{QQ} + H_{QP}G_P^{(+)}(E)H_{PQ} \quad , \quad (2)$$

where  $G_P^{(+)}(E)$  is a Green function for the motion of a single nucleon in  $P$ . The energy scale is settled by the one-nucleon emission threshold  $E^{(\text{thr})}$  [27]. For  $E > E^{(\text{thr})}$ ,  $\mathcal{H}$  is a complex-symmetric matrix, while for  $E < E^{(\text{thr})}$  it is hermitian like in the ordinary SM. The ground state (g.s.) continuum coupling correction to the binding energy is given by [28]:

$$E_{\text{corr}} = \langle \Phi_{\text{g.s.}} | \mathcal{H} - H_{QQ} | \Phi_{\text{g.s.}} \rangle. \quad (3)$$

The g.s. wave function in the parent nucleus ( $N, Z$ ) is coupled to different channel wave functions, which are determined by the motion of an unbound neutron relative to the daughter nucleus ( $N - 1, Z$ ) in a certain SM state  $\Phi_i^{(N-1)}$ . Figure 3 shows the neutron number dependence of  $E_{\text{corr}}$  in oxygen isotopes for (i)  $E_n^{(\text{thr})}$  of SMEC (solid line), and for (ii)  $E_n^{(\text{thr})}$  fixed arbitrarily at 0 or 4 MeV. In the present studies, we use the full  $sd$  valence space for  $N < 20$ , and the full  $pf$  space for  $N > 20$ . All asymptotic channels composed of SM states are included in these studies.

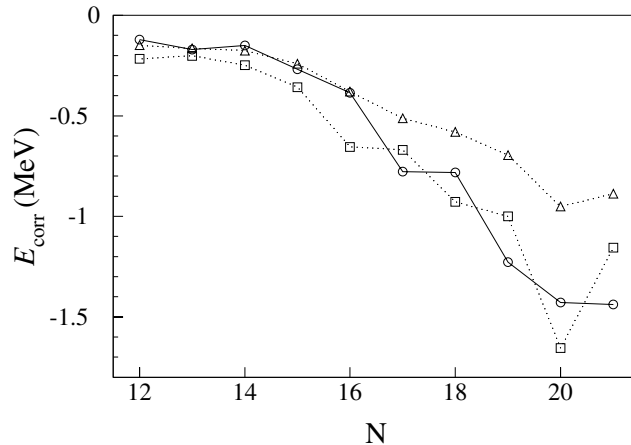


Figure 3: Neutron number dependence of  $E_{\text{corr}}$  (3) to the SM g.s. energy for neutron-rich oxygen isotopes. The solid line is obtained for one-neutron emission threshold  $E_n^{(\text{thr})}$  calculated in SMEC for each nucleus. The dotted lines with squares and triangles are obtained for  $E_n^{(\text{thr})}$  fixed at 0 and 4 MeV, respectively (from Ref. [28]).

A non-linear average behavior of  $E_{\text{corr}}(N)$ , seen in Fig. 3, has a double origin. For a fixed value of  $E_n^{(\text{thr})}$ , the continuum coupling induces an effective

change  $\delta V_{j_1 j_2}^{T=1} \sim (V^{(nn)})^2 / V_{j_1 j_2}^{T=1}$  of the  $T = 1$  matrix elements of the two-body interaction  $V_{j_1 j_2}^{T=1}$ . This dependence, which is well seen for the matrix elements involving the  $0d_{3/2}$  orbit, can be taken into account by a phenomenological correction of the  $T = 1$  two-body monopole terms in the effective two-body interaction. More important is the change of the average behavior of  $E_{\text{corr}}$  due to the strong dependence of  $E_{\text{corr}}$  on  $E_n^{(\text{thr})}$ . Close to the neutron drip line, this dependence leads to an effective enhancement of the strength of the  $nn$ -continuum coupling which cannot be corrected by the  $N$ -independent phenomenological correction of the two-body monopole terms.  $N$ -dependence of the two-body monopoles has been also recently advocated by Zuker [29] as a result of an approximation of the monopoles of the realistic interactions including a three-body force in the standard framework of the standard SM. Figure 3 clearly demonstrates that the  $N$ -dependence of the monopole Hamiltonian may have different physical origins and, in particular, it comes about quite naturally as a result of the coupling between  $Q$  and  $P$  subspaces. On top of this average behavior, one can see an odd-even staggering (OES) of  $E_{\text{corr}}(N)$ . In particular, the OES near the one-neutron drip line (see the curve for  $E_n^{(\text{thr})} = 0$ ) is a salient feature of the  $T = 1$  continuum coupling. If  $E_n^{(\text{thr})}$  is calculated in SMEC for each nucleus, the OES is inverted because  $E_n^{(\text{thr})}$  in an odd- $N$  nucleus is smaller than in even- $N$  neighbors.

## 5.2 Gamow Shell Model

Recently, the multiconfigurational CSM in the complete Berggren basis, the so-called Gamow Shell Model (GSM), has been formulated [30, 31]. The s.p. basis of GSM is given by the Berggren ensemble [32] which contains Gamow states (or resonant states and the non-resonant continuum).

The resonant states are the generalized eigenstates of the time-independent Schrödinger equation which are regular at the origin and satisfy purely outgoing boundary conditions. They correspond to the poles of the  $S$  matrix in the complex energy plane lying on or below the positive real axis. One may see here a two-subspace concept of Feshbach reappearing, with the subspace  $Q_B$  consisting of the Gamow states in the complex energy plane, and the subspace  $P_B$  containing the non-resonant continuum. In the GSM framework, the number of particles in the scattering continuum is not predetermined, but it results from a variational calculation in the Hilbert space spanned by all Slater determinants in  $Q_B$  and  $P_B$  subspaces. Hence, GSM can also be applied to Borromean systems for which  $A$ - and  $(A - 2)$ -nucleon systems are particle-stable but the intermediate  $(A - 1)$ -system is not. GSM is a natural

generalization of the SM concept for the open quantum systems. And, as such, it is a tool *par excellence* for nuclear structure studies. A description of many-body wave functions at large distances, as needed in nuclear reaction studies, even though feasible within the GSM formalism, may be rather cumbersome. For that purpose, the coupled-channel method used in SMEC to describe the asymptotic channels is far more accurate.

### 5.3 Completeness relation involving Gamow states

There exist several completeness relations involving resonant states. In the heart of GSM is the Berggren completeness relation [32] :

$$\sum_n |u_n\rangle\langle\tilde{u}_n| + \int_{L_+} |u_k\rangle\langle\tilde{u}_k| dk = 1 \quad , \quad (4)$$

where  $|u_n\rangle$  are the Gamow states (both bound states and the decaying resonant states lying between the real  $k$ -axis and the complex contour  $L_+$ ) and  $|u_k\rangle$  are the scattering states on  $L_+$ . The resonant states are normalized according to the squared radial wave function and not to the modulus of the squared radial wave function. This is a consequence of the analytical continuation which is used to introduce the normalization of Gamow states. In practical applications, one has to discretize the integral in (4). Such a discretized Berggren relation is formally analogous to the standard completeness relation in a discrete basis of  $L^2$ -functions and, in the same way, leads to the eigenvalue problem  $H|\Psi\rangle = E|\Psi\rangle$ . However, as the formalism of Gamow states is non-hermitian, the matrix  $H$  is complex symmetric. The discretized Berggren basis can be a starting point for establishing the completeness relation in the many-body case in full analogy with the standard SM in a complete (discrete) basis of  $L^2$ -functions. One obtains :

$$\sum_n |\Psi_n\rangle\langle\tilde{\Psi}_n| \simeq 1 \quad , \quad (5)$$

where  $|\Psi_n\rangle \equiv |\phi_1 \cdots \phi_N\rangle$  are the  $N$ -body Slater determinants, and  $|\phi_m\rangle$  are the resonant (bound and decaying) and scattering (contour) s.p. states. The approximate equality in Eq. (5) is a consequence of the continuum discretization. As in the case of s.p. Gamow states, the normalization of Gamow-Slater determinants is given by the squares of SM amplitudes :  $\sum_n c_n^2 = 1$  and not by the squares of their absolute values.

## 5.4 Determination of many-body bound and resonance states

In a standard SM, one often uses the Lanczos method to find the low-energy eigenstates (bound states) in very large configuration spaces. This popular method is unfortunately useless for the determination of many-body resonances because of a huge number (continuum) of surrounding many-body scattering states, many of them having lower energy than the resonances. A practical solution to this problem is the following procedure [30]:

- In the first step, one performs the pole approximation; i.e., the Hamiltonian is diagonalized in a smaller basis consisting of s.p. resonant states only. Here, some variant of the Lanczos method can be applied. The diagonalization yields the first-order approximation to many-body resonances  $|\Psi_i\rangle^{(0)}$ , where index  $i$  ( $i = 1, \dots, N$ ) enumerates all eigenvectors in the restricted space. These eigenvectors serve as starting vectors (pivots) for the second step of the procedure.
- In the second step, one includes couplings to non-resonant continuum states in the Lanczos subspace generated by  $|\Psi_j\rangle^{(0)}$  ( $j \in [1, \dots, N]$ ).
- Finally, one searches among the  $M$  solutions  $|\Psi_{j;k}\rangle$ , ( $k = 1, \dots, M$ ), for the eigenvector which has the largest overlap with  $|\Psi_j\rangle^{(0)}$ .

## 5.5 Example of the eigenvalue spectrum in $^{20}\text{O}$

In the following, we shall show that this procedure allows for an efficient determination of physical states within the set of all eigenvectors of a given Lanczos subspace. Figure 4 shows the GSM eigenvalue spectrum in the complex energy plane for the  $0^+$  states of  $^{20}\text{O}$ . While the two lowest (bound) states can be simply identified by inspection, for the higher-lying states it is practically impossible to separate the resonances from the non-resonant continuum. However, the procedure outlined above makes it possible to identify unambiguously the many-body resonance states.

The many-body resonances should be stable with respect to small deformations of the contour; i.e., they should not depend on the deformation of the basis. This observation offers an independent criterion for identifying resonance states. Fig. 5 shows the effect of a small deformation of the contour on the stability of selected  $0^+$  states in  $^{20}\text{O}$ . As expected, only the states which have previously been identified as resonances are stable with respect to small changes of the contour; the states belonging to the non-resonant continuum ‘walk’ in the complex energy plane following the contour’s motion.

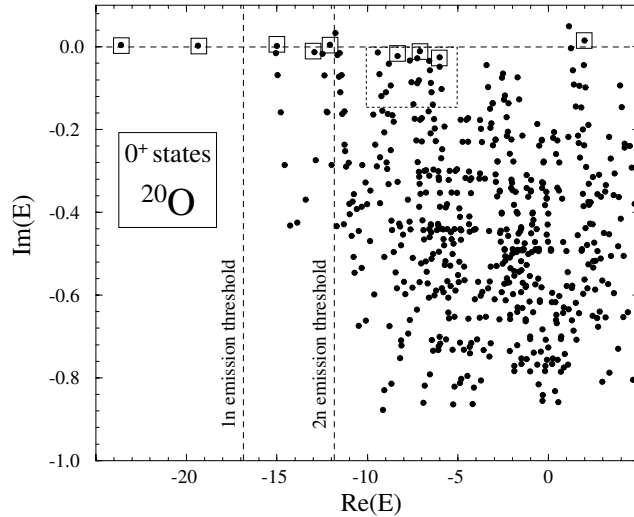


Figure 4: Complex energies of the  $0^+$  states in  $^{20}\text{O}$  obtained by the diagonalization of the GSM Hamiltonian. One- (1n) and two-neutron (2n) emission thresholds are indicated. The physical bound and resonance states are matched by squares. The remaining eigenstates represent the non-resonant continuum (from Ref. [31]).

## 5.6 GSM Study of Helium Isotopes

A description of neutron-rich helium isotopes, including Borromean nuclei  $^{6,8}\text{He}$ , is a challenging theoretical problem. The nucleus  $^4\text{He}$  is a well-bound system with the one-neutron emission threshold at 20.58 MeV. On the contrary, the nucleus  $^5\text{He}$  is a broad resonance. The nucleus  $^6\text{He}$ , which consists of two neutrons outside  $^4\text{He}$ , is bound with the two-neutron emission threshold at 1.87 MeV. The first excited  $2_1^+$  state in  $^6\text{He}$  at 1.8 MeV is neutron-unstable with a width  $\Gamma = 113$  keV.

In our GSM calculations, the s.p. configuration space includes both resonances  $0p_{3/2}$ ,  $0p_{1/2}$  and the two associated complex continua  $p_{3/2}$  and  $p_{1/2}$  which are discretized with 5 points each. At present, the principal limitation of GSM is due to the explosion of the number of configurations as compared to the standard SM. For each Gamow state (bound or resonant) of quantum numbers  $(\ell, j)$  in the single-particle basis, one should include the corresponding discretized continuum, i.e., instead of dealing with one shell  $(\ell, j)_i$ ; one has to consider a set of shells  $[(\ell, j)^{(c_1)}, (\ell, j)^{(c_2)}, \dots, (\ell, j)^{(c_n)}]$ , where  $n$  is the number of points along the discretized contour  $(\ell, j)$ . The possibility of dealing with this problem is to adopt the techniques borrowed from the Density Matrix Renormalization Group method [33]. Figure 6 shows the lowest energy

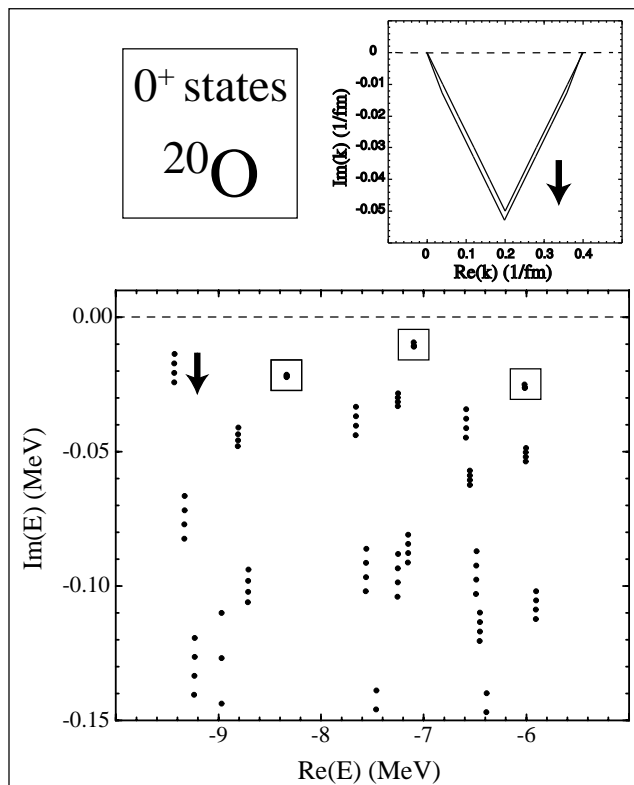


Figure 5: The effect of small changes in the contour on the stability of resonant and non-resonant  $0^+$  states in  $^{20}\text{O}$ . Top: the contour in the complex- $k$  plane corresponding to the  $0d_{3/2}$  continuum. The direction of the contour's deformation is indicated by an arrow. The calculations were performed for four contours, each divided into nine segments; only the first and maximally-deformed contours are shown. Bottom: the resulting shifts in positions of many-body states corresponding to the complex energy region of Fig. 4 marked by a dotted line. It is seen that the states identified as resonant are very stable with respect to small changes of the contour while the states representing the non-resonant continuum move significantly in the direction indicated by an arrow (from Ref. [31]).

states of helium isotopes calculated with the surface delta interaction with the strength  $V_{SDI} = 1670 \text{ MeV}\cdot\text{fm}^3$ . The  $0p_{3/2}$ ,  $0p_{1/2}$  s.p. resonances are generated by a Woods-Saxon potential with the parameters chosen to reproduce experimental energies and widths of the  $3/2_1^-$  and  $1/2_1^-$  resonances of  $^5\text{He}$ .

It is found that the non-resonant continuum contributions are *always essential* and, in some cases (e.g.,  $^8,^9\text{He}$ ), they dominate the structure of the g.s. wave function. Moreover, the wave function components having many neutrons in the non-resonant continuum give an essential contribution to the binding

energy. Without the non-resonant (contour) states, the predicted g.s. energy of  ${}^8\text{He}$  is  $+2.08$  MeV. The inclusion of scattering states lowers the binding energy to  $-1.6$  MeV. GSM calculations reproduce the most important feature of  ${}^{6,8}\text{He}$ : *the ground state is particle bound, despite the fact that all the basis states lie in the continuum*. The odd- $N$  isotopes of  ${}^{7,9}\text{He}$  are calculated to be wide

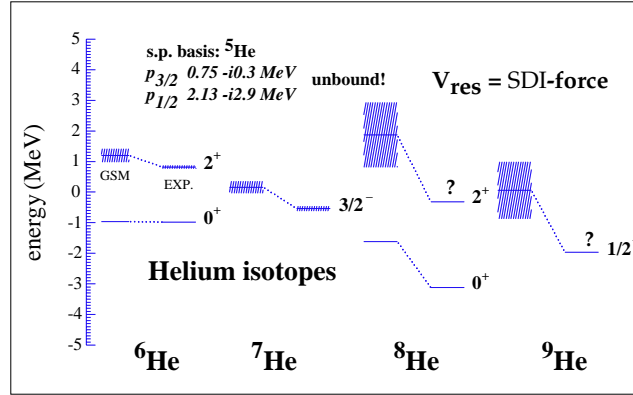


Figure 6: Experimental (EXP) and calculated (GSM) binding energies of  ${}^{6-9}\text{He}$  as well as energies of  $J^\pi = 2^+$  states in  ${}^6\text{He}$  and  ${}^8\text{He}$ . The resonance widths are indicated by shading. The energies are given with respect to the core of  ${}^4\text{He}$ .

neutron resonances. The neutron separation energy anomaly, i.e., the *increase* of one-neutron separation energy when going from  ${}^6\text{He}$  to  ${}^8\text{He}$ , is reproduced. This anomaly is explained in GSM by a large contribution from non-resonant continuum states. This generic mechanism, expected to be present in loosely bound systems, may give rise to the formation of multineutron Borromean systems, changing the *drip line* into a porous *drip zone*.

## 6 Conclusions

The main objective of this brief review was to discuss various challenges in theoretical nuclear structure, especially in the context of RNB physics. There are many unique features of exotic nuclei that give prospects for entirely new phenomena likely to be different from anything we have observed to date. New-generation data will be crucial in pinning down a number of long-standing questions related to the effective Hamiltonian, nuclear collectivity, and properties of nuclear excitations.

The material contained in this paper was obtained in collaboration with J. Dobaczewski, N. Michel, J. Okołowicz, M. Stoitsov, and J. Terasaki. This work

was supported in part by the U.S. Department of Energy under Contract Nos. DE-FG02-96ER40963 (University of Tennessee) and DE-AC05-00OR22725 with UT-Battelle, LLC (Oak Ridge National Laboratory).

## References

- [1] J. Dobaczewski and W. Nazarewicz, *Phil. Trans. R. Soc. Lond. A* **356**, 2007 (1998).
- [2] R. Machleidt, *Nucl. Phys. A* **689**, 11c (2001).
- [3] D.R. Entem and R. Machleidt, *Phys. Lett.* **524B**, 93 (2002).
- [4] S. Bogner, T.T.S. Kuo, L. Coraggio, A. Covello, and N. Itaco, *Phys. Rev. C* **65**, 051301 (2002).
- [5] E. Epelbaum, A. Nogga, W. Glockle, H.Kamada, Ulf.-G.Meissner, and H. Witala, *Phys. Rev. C* **66**, 064001 (2002).
- [6] S.C. Pieper and R.B. Wiringa, *Ann. Rev. Nucl. Part. Sci.* **51**, 53 (2001).
- [7] C.J. Pethick and D.G. Ravenhall, *Annu. Rev. Nucl. Part. Sci.* **45**, 429 (1995).
- [8] C. Horowitz and J. Piekarewicz, *Phys. Rev. Lett.* **86**, 5647 (2001).
- [9] R.J. Furnstahl, *Nucl. Phys. A* **706**, 85 (2002).
- [10] *Scientific Opportunities With an Advanced ISOL Facility*, Report, November 1997; <http://www.er.doe.gov/production/henp/isolpaper.pdf>.
- [11] J. Morales, V.R. Pandharipande, and D.G. Ravenhall, *Phys. Rev. C* **66**, 054308 (2002).
- [12] J. Carlson, J. Morales Jr., V.R. Pandharipande, and D.G. Ravenhall, *nucl-th/0302041* (2003).
- [13] J. Dobaczewski, W. Nazarewicz, and M. V. Stoitsov, *Eur. Phys. J. A* **15**, 21 (2002).
- [14] S. Goriely, M. Samyn, P.H. Heenen, J.M. Pearson, and F. Tondeur, *Phys. Rev. C* **66**, 024326 (2002).
- [15] M.V. Stoitsov, J. Dobaczewski, W. Nazarewicz, and J. Terasaki, in preparation.
- [16] M.V. Stoitsov, W. Nazarewicz, and S. Pittel, *Phys. Rev. C* **58**, 2092 (1998).

- [17] M.V. Stoitsov, J. Dobaczewski, P. Ring, and S. Pittel, *Phys. Rev. C* **61**, 034311 (2000).
- [18] J.A. Sheikh and P. Ring, *Nucl. Phys. A* **665**, 71 (2000).
- [19] J.A. Sheikh, P. Ring, E. Lopes, and R. Rossignoli, *Phys. Rev. C* **66**, 044318 (2002).
- [20] T. Duguet and P. Bonche, nucl-th/0210055 and nucl-th/0210057.
- [21] M. Farine, J.M. Pearson, and F. Tondeur, *Nucl. Phys. A* **696**, 396 (2001).
- [22] M. Bender, J. Dobaczewski, J. Engel, and W. Nazarewicz, *Phys. Rev. C* **65**, 054322 (2002).
- [23] P.-G. Reinhard, *Z. Phys. A* **285**, 93 (1978); P.-G. Reinhard and K. Goeke, *Rep. Prog. Phys.* **50**, 1 (1987).
- [24] P.-G. Reinhard, D.J. Dean, W. Nazarewicz, J. Dobaczewski, J.A. Maruhn, and M.R. Strayer, *Phys. Rev. C* **60**, 014316 (1999).
- [25] J. Okołowicz, M. Płoszajczak, and I. Rotter, *Phys. Rep.* **374**, 271 (2003).
- [26] J. B. Ehrmann, *Phys. Rev.* **81**, 412 (1951); R.G. Thomas, *Phys. Rev.* **81**, 148 (1951).
- [27] K. Bennaceur, F. Nowacki, J. Okołowicz, and M. Płoszajczak, *Nucl. Phys. A* **651**, 289 (1999) and *A* **671**, 203 (2000).
- [28] Y. Luo, J. Okołowicz, M. Płoszajczak, and N. Michel, nucl-th/0201073.
- [29] A. Zuker, nucl-th/0209073 (2002).
- [30] N. Michel, W. Nazarewicz, M. Płoszajczak, and K. Bennaceur, *Phys. Rev. Lett.* **89**, 042502 (2002).
- [31] N. Michel, W. Nazarewicz, M. Płoszajczak, and J. Okołowicz, nucl-th/0302060.
- [32] T. Berggren, *Nucl. Phys. A* **109**, 265 (1968).
- [33] J. Dukelsky, this volume and references quoted therein.